Modern human alleles differentially regulate gene expression in brain tissues: implications for brain evolution

Alejandro Andirkó[1,2] and Cedric Boeckx[1,2,3,*]

[1]University of Barcelona
[2]University of Barcelona Institute of Complex Systems
[3]ICREA
[*]Corresponding author: cedric.boeckx@ub.edu

Abstract

The availability of high-coverage genomes of our extinct relatives, the Neanderthals and Denisovans, and the emergence of large, tissue-specific databases of modern human genetic variation, offer the possibility of probing the evolutionary trajectory of heterogenous structures of great interest, such as the brain. Here we cross two publicly available datasets, the GTEX cis-eQTL database (version 8) and an extended catalog of *Homo sapiens* specific alleles relative to the Neanderthal and Denisovan sequences to understand how nearly fixed *Sapiens*-derived alleles affect the regulation of gene expression across 15 structures. The list of variants obtained reveals enrichments in regions of the modern human genome showing putative signals of positive selection relative to archaic humans, points to associations with clinical conditions, and places the focus on specific structures such as the cerebellum and the Hypothalamus-Pituitary-Adrenal Gland axis. The directionality of regulation of these variants complements earlier findings about introgressed variants from archaics, and highlights the role of genes that deserve closer experimental attention.

1 Introduction

State-of-the-art geometric morphometric analysis on endocasts [1, 2, 3, 4, 5] have revealed significant differences between Neanderthal and *Homo sapiens* skulls that are most likely the result of differential growth of neural tissue. Specific regions of the cerebellum, parietal and temporal lobes appear to have expanded in the modern lineage. These changes may have had consequences for the evolution of modern human cognition. In addition, facial differences

between modern and archaic humans have been claimed to go hand in hand with a reduction of certain brain and neural crest-derived structures such as the Hypothalamus-Pituitary-Adrenal Gland axis [6, 7].

Probing the nature of these differences directly, by looking at differences in brain tissue, is challenging, but the availability of several high-quality archaic genomes [8, 9, 10] has opened numerous research avenues and opportunities for studying the evolution of the *Homo sapiens* brain with unprecedented precision. Apart from the possibility of introducing specific archaic variants in model organisms both *in vivo* (transgenic mouse models) and *in vitro* (brain organoids) [11], researchers have explored the idea of connecting variation in modern human genomes data and brain evolution. A major study [12] explored the effects of Neanderthal and Denisovan introgressed variants in 44 tissues and found downregulaton by introgressed alleles in the brain, particularly in the cerebellum and the striatum. In a similar vein, another study [13] examined the effects of archaic introgression on brain and skull shape variability in a modern human population to determine which variants are associated with the globularized brain/skull that is characteristic of anatomically modern humans. Here too, the variants with the most salient effects were those found to affect the structure of the cerebellum and the striatum.

Building on these efforts, we chose to focus on the effects of derived, modern-specific alleles, as opposed to introgressed archaic alleles. To this end, we took advantage of a recent systematic review of high frequency changes in modern humans [14], which provides an exhaustive database of derived, *Homo sapiens*-specific alleles found at very high frequencies in modern human populations ($\geq$90% fixation). Because they are nearly fixed, these alleles can be compared to ancestral variants found at very low frequencies in modern genomes. To determine the predicted effect on gene expression of these derived, modern human-specific alleles, we exploited the GTEX database (version 8), which offers data for the following tissues of interest: Adrenal Gland, Amygdala, Caudate, Brodmann Area (BA) 9, BA24, Cerebellum, Cerebellar Hemisphere, Cortex, Hippocampus, Hypothalamus, Nucleus Accumbens, Pituitary, Putamen, Spinal Cord, and Substantia Nigra. Of these samples, cerebellar hemisphere and the cerebellum, as well as cortex and BA9, are to be treated as duplicates [15]. Though not a brain tissue *per se*, the adrenal gland was included due to its role in the Hypothalamic-pituitary-adrenal (HPA) axis, an important regulator of the neuroendocrine system that affects behavior.

We wish to stress that our focus on brain(-related) structures in no way is intended to claim that only the brain is the most salient locus of difference between moderns and archaics. While other body parts undoubtedly display derived characteristics, we have concentrated on the brain here because our primary interest lies in cognition and behavior, which is most directly affected by brain-related changes.

The GTEx data consist of statistically significant allele effects on gene expression dosage in single tissues, obtained from tissues of adult individuals aged 20 to 60 [15]. By offering information about Expression Quantitative Trait Loci (cis-eQTLs) across tissues, the GTEx database forces us to think beyond vari-

ants that affect the structure and function of proteins, as well as to consider those that regulate gene expression. Early efforts tried to determine the molecular basis of archaic-modern differences based on the few missense mutations that are *Homo sapiens*-specific [16]. But evidence is rapidly emerging in favor of an important evolutionary role of regulatory variants, as originally proposed more than four decades ago [17]. For instance, selective sweep scans to detect areas of the genome that have been significantly affected by natural selection after the split with Neanderthals show that regulatory variants played a prominent role [18]. Likewise, changes in potential regulatory elements have been singled out in attempts to identify the factors that gave the modern human face its shape [6, 19]. Other approaches, exploiting biobank data [20], have also stressed differences in gene regulatory architecture between modern humans and archaic hominins. Our study contributes to this emerging literature and highlights novel regulatory changes that deserve further experimentation.

2 Results

Our primary data source was the dataset in [14] that determines *Homo sapiens* allele specificity using the three high-coverage archaic human genomes, including the Altai [8] and Vindija [9] Neanderthals, and a high-quality sequence of the genome of a Denisovan [10], as well as chimpanzee and macaque data to determine which allele was derived or ancestral. We adopted the filtering criteria ($\geq$90% allele frequency) established in the original study [14], but, departing from the original article data, we decided to restrict our attention to those derived alleles found at high frequency ($\geq$90% fixation) not only globally, but in each of the major human populations (see section 4). We then crossed the list of variants obtained with the GTEX v8 data to determine which of these alleles significantly affected gene expression, focusing on the 15 tissues mentioned above. We further integrated our data with a curated collection of all published genome-wide association studies, produced by a collaboration between EMBL-EBI and NHGRI [21], the Clinvar database [22], as well as other genomic regions identified as being of interest for human evolution, such as regions showing signals of putative positive selection [18, 23] or deserts of introgression (regions depleted of introgressed variants) [24].

2.1 eQTL numbers and distribution

The resulting dataset is composed of *Homo sapiens* derived alleles at high frequency that have a statistically significant effect on gene expression in any of the adult human tissues we selected. This includes 8,271 statistically significant unique SNPs associated with the regulation of a total of 896 eGenes (i.e., genes affected by cis-regulation) (Figure 1). The total number of eQTLs in the processed dataset correlates moderately with chromosome size ($r = 66$; $p = 0.00053$, Pearson correlation test). Chromosome Y is not included in the analysis due to the lack of Y chromosomes in the archaic samples. Among eQTLs, intron

variants are over-represented (Figure 2). We identified one stop loss in *PSPN* (persephin neurothropic factor) (rs80336323), 16 splice region variants and 47 missense variants (Figure 2), including one in *PCNT*, a gene that we return to in section 2.3. Transcription start site (TSS) distance approximates a normal distribution, as shown in Figure 2. We find some degree of functional overlap among eQTLs: 161 eQTLs regulate various genes in the same tissue or across different tissues. The tissue with the highest number of tissue-specific eQTLs is the pituitary, followed by the cerebellum and the adrenal gland (Figure 3).

Because eQTL mapping is highly dependent on the number of samples [25], we sought to determine if there was a tendency of tissues with more samples to have a higher number of significant variants (Figure 3). We found that there is indeed a linear correlation ($p = 0.00057$; $r = 0.78$, Pearson correlation test) between sample size and number of significant variants. Nonetheless we discovered that the cerebellum stood out in containing a high number of expression-affecting variants relative to its sample size and to other tissues. A Principal Component Analysis of the data revealed that there is a correlation between minor allele frequency and minor allele samples in the GTEx database (Supplementary Figure S1). Given that brain samples are hard to obtain, this correlation signals that the rarer the allele the more likely a given eQTL locus is to be undersampled.

Concerning directionality of expression, regulated by identified variants, there is an overall tendency for ancestral alleles to downregulate gene expression (Figure 3). This tendency is particularly prominent in the Substantia Nigra. We performed a binomial exact test to determine if this deviation was significant, and found this to be the case ($p < 0.05$) in all tissues except for 'Cortex', 'Hypothalamus' and 'Nucleus Accumbens'. A previous study looking at the effect of introgressed variants on gene expression [12] had suggested that (introgressed) Neanderthal alleles downregulate gene expression in the brain and testes. As far as the brain is concerned, this observation (generalized to archaic variants) also obtains in our study, with the added result that there seems to be brain-tissue-dependent variability in the degree of downregulation when the derived eQTL is found in high frequency.

In order to control for linkage disequilibrium, we clumped the variants from our database around the allele with the lowest p-value in eQTL mapping. This reduced the total number of variants in our data to 4,128, out of which 1,336 are tissue-specific. Among the eGenes with the strongest effects across tissues (top 5%), one finds *METTL14*, present in cerebellar, cortex and pituitary samples. *METTL14*, along with *METTL3*, is part of a complex that regulates expression of N6-methyladenosine (m6a), an epitranslational RNA modifier that has been shown to have an important role in cerebellar development in mice [26]. *METTL14* also plays a role in oligodendrocyte maturation and myelination [27], as well as in extending neurogenesis to postnatal developmental stages [28]. Among the eGenes that emerged after clumping we also find other genes related to neurodevelopment, such as *NUDC*, necessary for neuronal migration [29], and *PIGV*, associated with Hyperphosphatasia-mental retardation syndrome [30].

Tissue	Molecular process	Transcription factor
Caudate	Cytosol	-
Cerebellar hemisphere, Cerebellum	-	E2F-4
BA9	-	N-Myc
Hippocampus	TCA Cycle and Deficiency of Pyruvate Dehydrogen	-
Putamen	Melanin biosynthesis	-
Substantia Nigra	Cell-cell adhesion, integral component of plasma membrane, ion binding	HOXB8

Table 1: A summary of Gene Ontology analysis results per tissue after variant clumping.

rsID	Gene	Clinical condition
rs17643644	*SF3B4*	Nager Syndrome
rs17801742	*COL2A1*	Stickler Syndrome
rs34500739	*PCNT*	Microcephalic primordial dwarfism
rs79305633	*RYR3*	Epileptic encephalopathy

Table 2: Benign variants in our database that were associated in Clinvar with craniofacial and bone atypical development. The full list can be found in Supplementary Table S2.

2.2 Enrichment analysis

Using the clumped subset of variants, we performed a GO enrichment analysis for each of the 15 tissues' top variants (selected results discussed in Table 1). We found an enrichment in transcription factors related to brain development. *E2F-4* is enriched in both cerebellar tissues included in this study. *E2F-4* knockout mice show developmental delay of the cerebellum, as well as abnormal craniofacial development, through disregulation of the Sonic Hedhehog (Shh) pathway [31]. *N-Myc*, enriched in Brodmann Area 9, is necessary for typical neuronal development [32]. In the Substantia Nigra we report an enrichment for the *HOXB8* transcription factor, which has been related to OCD-like behavior in mice through alterations in corticostriatal circuitry [33].

At the cell level we found enrichments for neuromelanin biosynthesis, argued to be related to neuroprotection and aging diseases [34] as well as ion binding, a key physiological function disrupted in Parkinson's Disease in the Substantia Nigra [35]. Other results, such as an enrichment in Pyruvate Dehydrogen deficiency in the hippocampus, also point to neurodegeneration as an important factor, as Pyruvate is known to protect against Alzheimer's disease [36] and the Hippocampus is one of the main tissues affected by the disease [37].

2.3 Clinical data and GWAS

Out of the clumped data, a total number of 11 variants were assigned a benign association with clinical conditions in Clinvar [22]. While this means there was no Mendelian association between these variants and the appearance of these conditions, they do affect the expression of the genes associated with the clinical phenotype, even if not to the point of causing atypical development. We find that several of these associations are related to collagen development: reduced levels of *SF3B4*, a regulator of transcription, have been associated with collagen

secretion problems [38]; *COL2A1* and *PCNT* are known to affect craniofacial development [39, 40]; *RYR3* is part of the family of ryanodine receptors that regulate calcium metabolism in bone [41]. In the NHGRI-EMBI GWAS catalog [21] we found that a variant of *COL2A1* was also the top result of a GWAS height study [42]. Interestingly, a variant that lies in *BAZ1B*, a gene related to craniofacial development in human evolution and part of the Williams-Beuren Syndrome critical region [6], was found to be one of the top results of a GWAS that measured infant head circumference [43]. This variant affected gene expression in cerebellar tissue in our data. We also found four variants associated to cognitive phenotypes: myelination [44], loneliness [45] and autism [46] (see Supplementary Table S1 for the full results).

2.4 Regions of evolutionary significance

To further determine the evolutionary significance of any of the genes that are affected by regulation in our data, we tested whether whether the eQTLs, or genes regulated by them, fell within positively selected regions of the genome in modern humans versus archaics ([18, 23]). We ran two randomization and permutation tests ($N = 10,000$) with [47] to see if the SNPs accumulate significantly in regions under positive selection relative to archaic humans (Supplementary Figure S2).

We found a significant ($p < 0.0013$) overlap between eQTLs and regions of positive selection as defined by [18]. There was also significant overlap with an earlier independent study identifying regions under positive selection ($p < 0.015$) [23]. The permutation tests were done using the unclumped data (see section 4). A chi-square independence test showed that Adrenal Gland, Brodmann Area 24, Amygdala and Pituitary have a significantly larger amount of eQTLs under positive selection relative to the other tissues ($p < 0.05$ after Bonferroni correction). Other tissues such as the cerebellum also showed a significant deviation from the overall proportion, but only for one of the studies [18].

Some of the genes associated with signals of positive selection and affected by differential gene expression have already been linked to clinical phenotypes or brain development: for example, *NRG4* is involved in dendritic development [48]. RAB7A has been found to be related to tau secretion, a marker of Alzheimer's disease [49], and GABPB2 has been associated with schizophrenia [50]. The BAZ1B variant discussed in section 2.3 affects the expression of two genes that, like *BAZ1B* itself, are part of the Williams-Beuren Syndrome Critical Region (*MLXIPL* and *NSUN5P2*).

Additionally, we tested whether any of the eQTLs fell within deserts of introgression, i.e., genetic windows of at least 10 Mb that have resisted genetic flow from Neanderthals and Denisovans to *Homo sapiens* ([24]). While some eQTLs do fall within these regions, a permutation test showed that they are not significantly enriched for such variants ($p > 0.18$). We also explored whether derived eQTLs overlapped with any known human miRNA or miRNA seeds (as defined in [51]), but found no overlap with our data.

3 Discussion

In this study we sought to shed light on which brain regions may be evolutionarily more derived in modern humans compared to their closest extinct relatives by quantifying the extent of differential gene regulation caused by modern-human-specific (derived) alleles found at very high frequency. In so doing we hoped to complement previous work [12, 13] focusing on the effects of introgressed (archaic) variants.

Three regions stand out in our data: the cerebellum, pituitary, and adrenal gland, which exhibit the highest degrees of eQTL tissue-specificity (Figure 3). While it has been pointed out that the cerebellum has a particular methylation profile compared to the rest of the brain, possibly affecting eQTL detection [52, 53], this argument does not hold for the pituitary and adrenal gland. For these, tissue specificity may be due to them belonging to the neuroendocrine pathway. The cerebellum also stands out in our study in terms of the number of variants that it contains relative to its sample size, as evidenced in Figure 3. The distinctive character of the cerebellum, the pituitary and the adrenal gland could be taken as support for claims assigning a special status to the cerebellum and the HPA axis in the context of modern human evolution [3, 6, 7, 13].

We replicated the observation [12] that archaic variants tend to cause gene downregulation in the modern human brain. We note that in our study, this effect is brain tissue dependent (it does not obtain for Cortex, Hypothalamus, and Nucleus Accumbens). Moreover, our results may be affected in part by tissue sample size, as the tissue with the highest proportion of downregulation, the Substantia Nigra, is the tissue with the lowest number of samples (figure 3). Our study also supports the claim [18] that regulatory regions tend to be associated with signals of positive selection in modern humans, as we found that high-frequency variants detected as cis-eQTLs are significantly present in areas identified as positively selected in two independent studies. Cross-checking these variants with comprehensive GWAS and medical databases suggests that these may have had consequences for cognition.

In terms of candidate genes and processes, we wish to highlight the enrichment we found associated with the *E2F4* transcription factor in cerebellar tissue. *E2F4* is an important postmitotic neuroblast regulator in mice [48]. If this is also confirmed to be the case for humans, neuroblasts might have been affected by differential regulation in *Homo sapiens*. In terms of brain disorders, we also found enrichments for genes related to neurodegenerative diseases (section 2.2). It has been pointed out that the origin of these human-specific neurodegenerative diseases might be found in relatively recent evolutionary events [54, 55, 56]. It might be the case that some of these variants found at high frequency contribute to the genetic makeup underlying our susceptibility to neurodegeneration.

The genetic regulatory networks shared by both the brain and craniofacial complex are also reflected in the amount of *Homo sapiens* derived eQTLs in the brain linked to disorders that affect skull morphology (see section 2.3). In this context we want to highlight the relevance of *BAZ1B*, a gene that we have

previously shown to affect the characteristic *Homo sapiens* facial shape but whose implication in brain evolution is still poorly understood.

All in all, our work reinforces the potential of using human variation databases as a valuable point of entry to connect genotype and phenotype in brain evolution studies, and corroborates claims made on the basis of the (fragmented) fossil record concerning the mosaic nature of our brain's evolutionary trajectory.

4 Methods

We accessed the *Homo sapiens* variant annotation data from [14]. The original complete dataset is publicly available at `https://doi.org/10.6084/m9.figshare.8184038`. This dataset includes archaic-specific variants and all loci showing variation within modern populations. It also contains information on population frequency, rsIDs and allele ancestrality. For replication purposes, we wrote a script that reproduces the 90% frequency cutoff point in the original study. We filtered the variants according to the guidelines in [14] such that: 1) all variants show 90% allele frequency, 2) the major allele present in *Homo sapiens* is derived (ancestrality is either determined by the criteria in [57] or by the macaque reference allele), whereas either archaic reliable genotypes have the ancestral allele, or the Denisovan carries the ancestral allele and one of the Neanderthals the derived allele (accounting for gene flow from *Homo sapiens* to Neanderthal).

Additionally, the original study we relied on [14] applies the 90% frequency cutoff point in a global manner: it requires that the global frequency of an allele be more than or equal to 90%, allowing for specific populations to display lower frequencies. Using the metapopulation frequency information provided in the original study, we applied a more rigorous filter and removed any alleles that where below 90% in any of the five major metapopulations included (African, American, East Asian, European, South Asian). We then harmonized and mapped the high-frequency variants to the data provided by the GTEx database [25]. In order to do so we pruned out the alleles that did not have an assigned rsID.

Clumping of the variants to control for Linkage Disequilibrium was done with Plink (version 1.9), requiring a linkage disequilibrium score of 0.99 (i.e., co-inheritance in 99% of cases) for an SNP to be clumped. The p-value for the eQTL mapping was used as the criterion to define a top variant, in such a way that haplotypes were clumped around the most robust eQTL candidate variant. The linkage disequilibrium map was extracted from the 1000 Genomes project ftp server (`ftp://ftp.1000genomes.ebi.ac.uk/vol1/ftp/release/20130502/`) and is composed of a diverse panel of individuals from the five meta-populations mentioned above.

We performed the Gene Ontology analysis with the *gprofiler* R package [58]. We performed the permutation test (n=10,000) with the R package RegioneR [47] using the unclumped data, as variants might clump around an eQTL falling outside windows of putative positive selection, causing an underepresentation

of the number of data points inside such genomic areas. Figures were created with the ggplot2 R package [59], Circos [60] and RegioneR [47]. The miRNA data was extracted from the Supplementary Tables S6 and S7 of [51]. For the human selective sweep data we used Supplementary Table S5 from [23], and Supplementary Table S2 from [18]. For the deserts of introgression data we extracted the information from [24]: these tables, reformatted for the code of this article to be run, can be found in Supplementary Table S3. S3A, S3B and S3C correspond to

The complete code to reproduce the data processing, plot generation and analysis can be found in `https://github.com/AGMAndirko/GTEX-code`.

Acknowledgments

The Genotype-Tissue Expression (GTEx) Project was supported by the Common Fund of the Office of the Director of the National Institutes of Health, and by NCI, NHGRI, NHLBI, NIDA, NIMH, and NINDS. The data used for the analyses described in this manuscript were obtained from the GTEx Portal on 05/15/19.

Author Contributions

Conceptualization: CB & AA; Data Curation: AA; Formal Analysis: AA; Funding Acquisition: CB; Investigation: CB & AA; Methodology: CB & AA; Software: AA; Supervision: CB; Visualization: CB & AA; Writing — Original Draft Preparation: CB & AA; Writing — Review & Editing: CB & AA.

Funding statement

AA acknowledges financial support from the Spanish Ministry of Economy and Competitiveness and the European Social Fund (BES-2017-080366). CB acknowledges financial support from the Spanish Ministry of Economy and Competitiveness/FEDER (grant FFI2016-78034-C2-1-P), the Marie Curie International Reintegration Grant from the European Union (PIRG-GA-2009-256413), research funds from the Fundació Bosch i Gimpera,the MEXT/JSPS Grant-in-Aid for Scientific Research on Innovative Areas 4903 (Evolinguistics: JP17H06379), and support from the Generalitat de Catalunya (2017-SGR-341).

Competing interest

Authors declare no competing financial or non-financial interest.

References

[1] P. Gunz, *et al.*, "Brain development after birth differs between Neanderthals and modern humans," *Current Biology*, vol. 20, pp. R921–R922, Nov. 2010.

[2] J.-J. Hublin, *et al.*, "Brain ontogeny and life history in Pleistocene hominins," *Phil. Trans. R. Soc. B*, vol. 370, p. 20140062, Mar. 2015.

[3] S. Neubauer, *et al.*, "The evolution of modern human brain shape," *Sci. Adv.*, vol. 4, p. eaao5961, Jan. 2018.

[4] A. S. Pereira-Pedro, *et al.*, "A morphometric comparison of the parietal lobe in modern humans and Neanderthals," *Journal of Human Evolution*, vol. 142, p. 102770, May 2020.

[5] T. Kochiyama, *et al.*, "Reconstructing the Neanderthal brain using computational anatomy," *Scientific Reports*, vol. 8, p. 6296, Apr. 2018.

[6] M. Zanella, *et al.*, "Dosage analysis of the 7q11.23 Williams region identifies *BAZ1B* as a major human gene patterning the modern human face and underlying self-domestication," *Sci. Adv.*, vol. 5, p. eaaw7908, Dec. 2019.

[7] R. W. Wrangham, *The Goodness Paradox: The Strange Relationship between Virtue and Violence in Human Evolution*. New York: Pantheon Books, first edition ed., 2019.

[8] K. Prüfer, *et al.*, "The complete genome sequence of a Neanderthal from the Altai Mountains," *Nature*, vol. 505, pp. 43–49, Jan. 2014.

[9] K. Prüfer, *et al.*, "A high-coverage Neandertal genome from Vindija Cave in Croatia," *Science*, vol. 358, pp. 655–658, Nov. 2017.

[10] M. Meyer, *et al.*, "A High-Coverage Genome Sequence from an Archaic Denisovan Individual," *Science*, vol. 338, pp. 222–226, Oct. 2012.

[11] M. Dannemann, *et al.*, "Human stem cell resources are an inroad to Neandertal DNA functions," preprint, Evolutionary Biology, Apr. 2018.

[12] R. C. McCoy, *et al.*, "Impacts of Neanderthal-Introgressed Sequences on the Landscape of Human Gene Expression," *Cell*, vol. 168, pp. 916–927.e12, Feb. 2017.

[13] P. Gunz, *et al.*, "Neandertal Introgression Sheds Light on Modern Human Endocranial Globularity," *Current Biology*, vol. 29, pp. 120–127.e5, Jan. 2019.

[14] M. Kuhlwilm *et al.*, "A catalog of single nucleotide changes distinguishing modern humans from archaic hominins," *Sci Rep*, vol. 9, p. 8463, Dec. 2019.

[15] GTEx Consortium, "Genetic effects on gene expression across human tissues," *Nature*, vol. 550, pp. 204–213, Oct. 2017.

[16] S. Pääbo, "The Human Condition—A Molecular Approach," *Cell*, vol. 157, pp. 216–226, Mar. 2014.

[17] M. King *et al.*, "Evolution at two levels in humans and chimpanzees," *Science*, vol. 188, pp. 107–116, Apr. 1975.

[18] S. Peyrégne, *et al.*, "Detecting ancient positive selection in humans using extended lineage sorting," *Genome Res.*, vol. 27, pp. 1563–1572, Sept. 2017.

[19] D. Gokhman, *et al.*, "Differential DNA methylation of vocal and facial anatomy genes in modern humans," *Nat Commun*, vol. 11, p. 1189, Dec. 2020.

[20] L. L. Colbran, *et al.*, "Inferred divergent gene regulation in archaic hominins reveals potential phenotypic differences," *Nat Ecol Evol*, vol. 3, pp. 1598–1606, Nov. 2019.

[21] A. Buniello, *et al.*, "The NHGRI-EBI GWAS Catalog of published genome-wide association studies, targeted arrays and summary statistics 2019," *Nucleic Acids Research*, vol. 47, pp. D1005–D1012, Jan. 2019.

[22] M. J. Landrum, *et al.*, "ClinVar: Improving access to variant interpretations and supporting evidence," *Nucleic Acids Research*, vol. 46, pp. D1062–D1067, Jan. 2018.

[23] F. Racimo, *et al.*, "A Test for Ancient Selective Sweeps and an Application to Candidate Sites in Modern Humans," *Molecular Biology and Evolution*, vol. 31, pp. 3344–3358, Dec. 2014.

[24] S. Sankararaman, *et al.*, "The Combined Landscape of Denisovan and Neanderthal Ancestry in Present-Day Humans," *Current Biology*, vol. 26, pp. 1241–1247, May 2016.

[25] The GTEx Consortium, *et al.*, "The Genotype-Tissue Expression (GTEx) pilot analysis: Multitissue gene regulation in humans," *Science*, vol. 348, pp. 648–660, May 2015.

[26] C. Ma, *et al.*, "RNA m6A methylation participates in regulation of postnatal development of the mouse cerebellum," *Genome Biol*, vol. 19, p. 68, Dec. 2018.

[27] H. Xu, *et al.*, "m6A mRNA Methylation Is Essential for Oligodendrocyte Maturation and CNS Myelination," *Neuron*, vol. 105, pp. 293–309.e5, Jan. 2020.

[28] K.-J. Yoon, *et al.*, "Temporal Control of Mammalian Cortical Neurogenesis by m6A Methylation," *Cell*, vol. 171, pp. 877–889.e17, Nov. 2017.

[29] S. Cappello, *et al.*, "NudC is required for interkinetic nuclear migration and neuronal migration during neocortical development," *Developmental Biology*, vol. 357, pp. 326–335, Sept. 2011.

[30] D. Horn, *et al.*, "Delineation of PIGV mutation spectrum and associated phenotypes in hyperphosphatasia with mental retardation syndrome," *Eur J Hum Genet*, vol. 22, pp. 762–767, June 2014.

[31] V. A. Swiss *et al.*, "Cell-context specific role of the E2F/Rb pathway in development and disease," *Glia*, pp. NA–NA, 2009.

[32] P. S. Knoepfler, "N-myc is essential during neurogenesis for the rapid expansion of progenitor cell populations and the inhibition of neuronal differentiation," *Genes & Development*, vol. 16, pp. 2699–2712, Oct. 2002.

[33] J. M. Greer *et al.*, "Hoxb8 Is Required for Normal Grooming Behavior in Mice," *Neuron*, vol. 33, pp. 23–34, Jan. 2002.

[34] L. Zecca, *et al.*, "New melanic pigments in the human brain that accumulate in aging and block environmental toxic metals," *Proceedings of the National Academy of Sciences*, vol. 105, pp. 17567–17572, Nov. 2008.

[35] N. González, *et al.*, "Effects of alpha-synuclein post-translational modifications on metal binding," *J. Neurochem.*, vol. 150, pp. 507–521, Sept. 2019.

[36] X. Wang, *et al.*, "Systemic pyruvate administration markedly reduces neuronal death and cognitive impairment in a rat model of Alzheimer's disease," *Experimental Neurology*, vol. 271, pp. 145–154, Sept. 2015.

[37] K. Moodley *et al.*, "The Hippocampus in Neurodegenerative Disease," in *Frontiers of Neurology and Neuroscience* (K. Szabo *et al.*, eds.), vol. 34, pp. 95–108, Basel: S. KARGER AG, 2014.

[38] F. Xiong *et al.*, "SF3b4: A Versatile Player in Eukaryotic Cells," *Front. Cell Dev. Biol.*, vol. 8, p. 14, Jan. 2020.

[39] A. Rauch, *et al.*, "Mutations in the Pericentrin (PCNT) Gene Cause Primordial Dwarfism," *Science*, vol. 319, pp. 816–819, Feb. 2008.

[40] L. Guo, *et al.*, "Novel and recurrent COL11A1 and COL2A1 mutations in the Marshall–Stickler syndrome spectrum," *Hum Genome Var*, vol. 4, p. 17040, Dec. 2017.

[41] L. J. Robinson, *et al.*, "Regulation of bone turnover by calcium-regulated calcium channels: Regulation of bone turnover," *Annals of the New York Academy of Sciences*, vol. 1192, pp. 351–357, Apr. 2010.

[42] G. Kichaev, *et al.*, "Leveraging Polygenic Functional Enrichment to Improve GWAS Power," *The American Journal of Human Genetics*, vol. 104, pp. 65–75, Jan. 2019.

[43] X.-L. Yang, *et al.*, "Three Novel Loci for Infant Head Circumference Identified by a Joint Association Analysis," *Front. Genet.*, vol. 10, p. 947, Oct. 2019.

[44] W. D. Hill, *et al.*, "A combined analysis of genetically correlated traits identifies 187 loci and a role for neurogenesis and myelination in intelligence," *Mol Psychiatry*, vol. 24, pp. 169–181, Feb. 2019.

[45] J. Gao, *et al.*, "Genome-Wide Association Study of Loneliness Demonstrates a Role for Common Variation," *Neuropsychopharmacol*, vol. 42, pp. 811–821, Mar. 2017.

[46] "Identification of risk loci with shared effects on five major psychiatric disorders: A genome-wide analysis," *The Lancet*, vol. 381, pp. 1371–1379, Apr. 2013.

[47] B. Gel, *et al.*, "regioneR: An R/Bioconductor package for the association analysis of genomic regions based on permutation tests," *Bioinformatics*, p. btv562, Sept. 2015.

[48] B. Paramo, *et al.*, "An essential role for neuregulin-4 in the growth and elaboration of developing neocortical pyramidal dendrites," *Experimental Neurology*, vol. 302, pp. 85–92, Apr. 2018.

[49] L. Rodriguez, *et al.*, "Rab7A regulates tau secretion," *J. Neurochem.*, vol. 141, pp. 592–605, May 2017.

[50] S.-A. Lee *et al.*, "Epigenetic profiling of human brain differential DNA methylation networks in schizophrenia," *BMC Med Genomics*, vol. 9, p. 68, Dec. 2016.

[51] P. R. Branco, *et al.*, "Uncovering association networks through an eQTL analysis involving human miRNAs and lincRNAs," *Sci Rep*, vol. 8, p. 15050, Dec. 2018.

[52] S. K. Sieberts, *et al.*, "Large eQTL meta-analysis reveals differing patterns between cerebral cortical and cerebellar brain regions," preprint, Genetics, May 2019.

[53] L. M. F. Sng, *et al.*, "Genome-wide human brain eQTLs: In-depth analysis and insights using the UKBEC dataset," *Sci Rep*, vol. 9, p. 19201, Dec. 2019.

[54] E. Bufill, *et al.*, "Alzheimer's disease: An evolutionary approach," *Journal of Anthropological Sciences*, no. 91, pp. 135–157, 2013.

[55] A. Nitsche, *et al.*, "Alzheimer-related genes show accelerated evolution," *Mol Psychiatry*, Mar. 2020.

[56] E. Bruner *et al.*, "Alzheimer's Disease: The Downside of a Highly Evolved Parietal Lobe?," vol. 35, no. 2, pp. 227–240.

[57] B. Paten, *et al.*, "Genome-wide nucleotide-level mammalian ancestor reconstruction," *Genome Research*, vol. 18, pp. 1829–1843, Nov. 2008.

[58] U. Raudvere, *et al.*, "G:Profiler: A web server for functional enrichment analysis and conversions of gene lists (2019 update)," *Nucleic Acids Research*, vol. 47, pp. W191–W198, July 2019.

[59] H. Wickham, *Ggplot2: Elegant Graphics for Data Analysis*. Use R!, New York: Springer, 2009. OCLC: ocn382399721.

[60] M. Krzywinski, *et al.*, "Circos: An information aesthetic for comparative genomics," *Genome Research*, vol. 19, pp. 1639–1645, Sept. 2009.

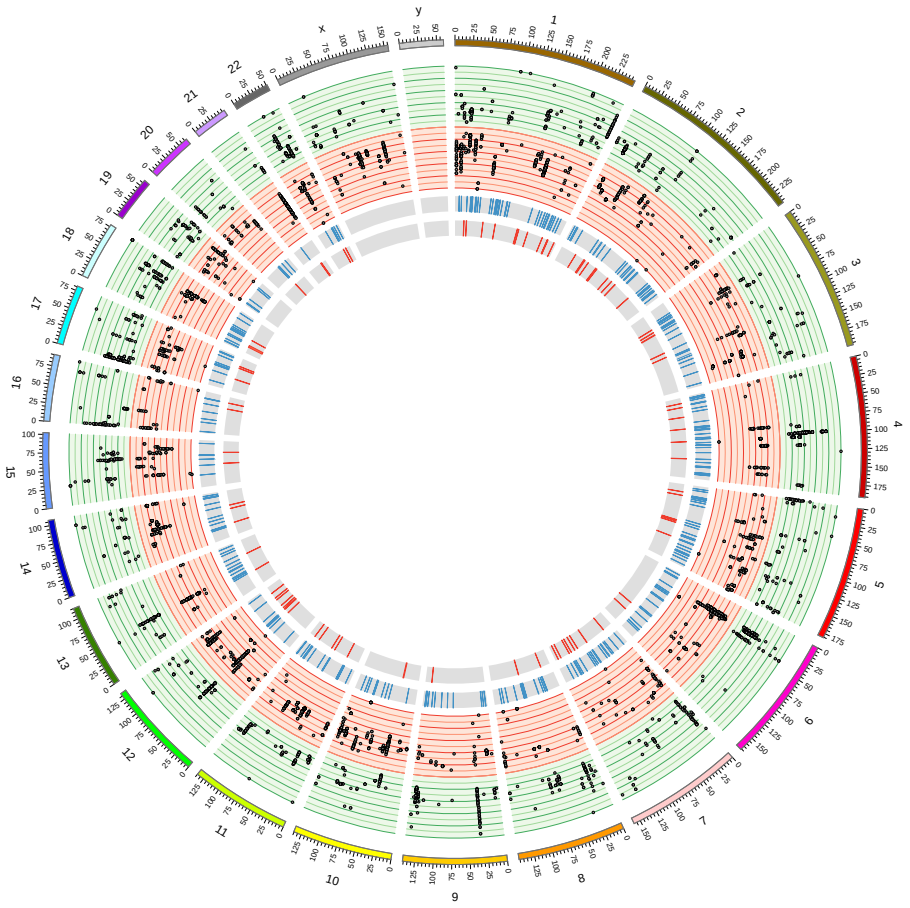

Figure 1: Circos plot showing the distribution along the genome of eQTLs. Each line denotes 0.5 steps in a gene expression normalized effect size, in a scale from 3 to -3. Red circles denote downregulation, green circles upregulation of eGenes. Inner rings: areas showing signals of positive selection relative to archaic humans in [18] (blue), and [23] (red).

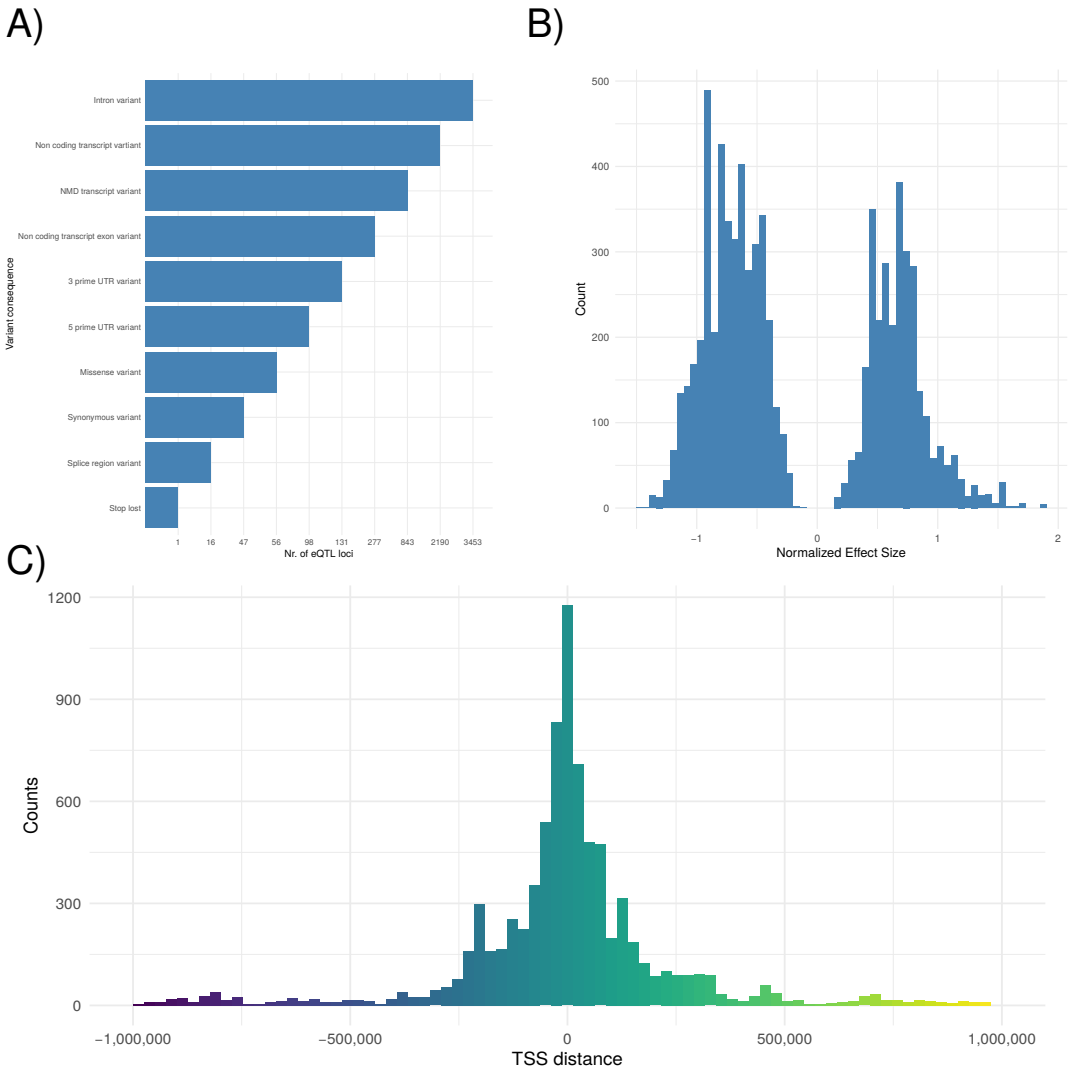

Figure 2: A) Barplot showing variant consequences of *Homo sapiens* cis-eQTL derived alleles, B) normalized effect size in gene expression across the 15 tissues, and C) distribution of eQTL distance to Transcription Starting Site (TSS). Figures A-C generated before clumping.

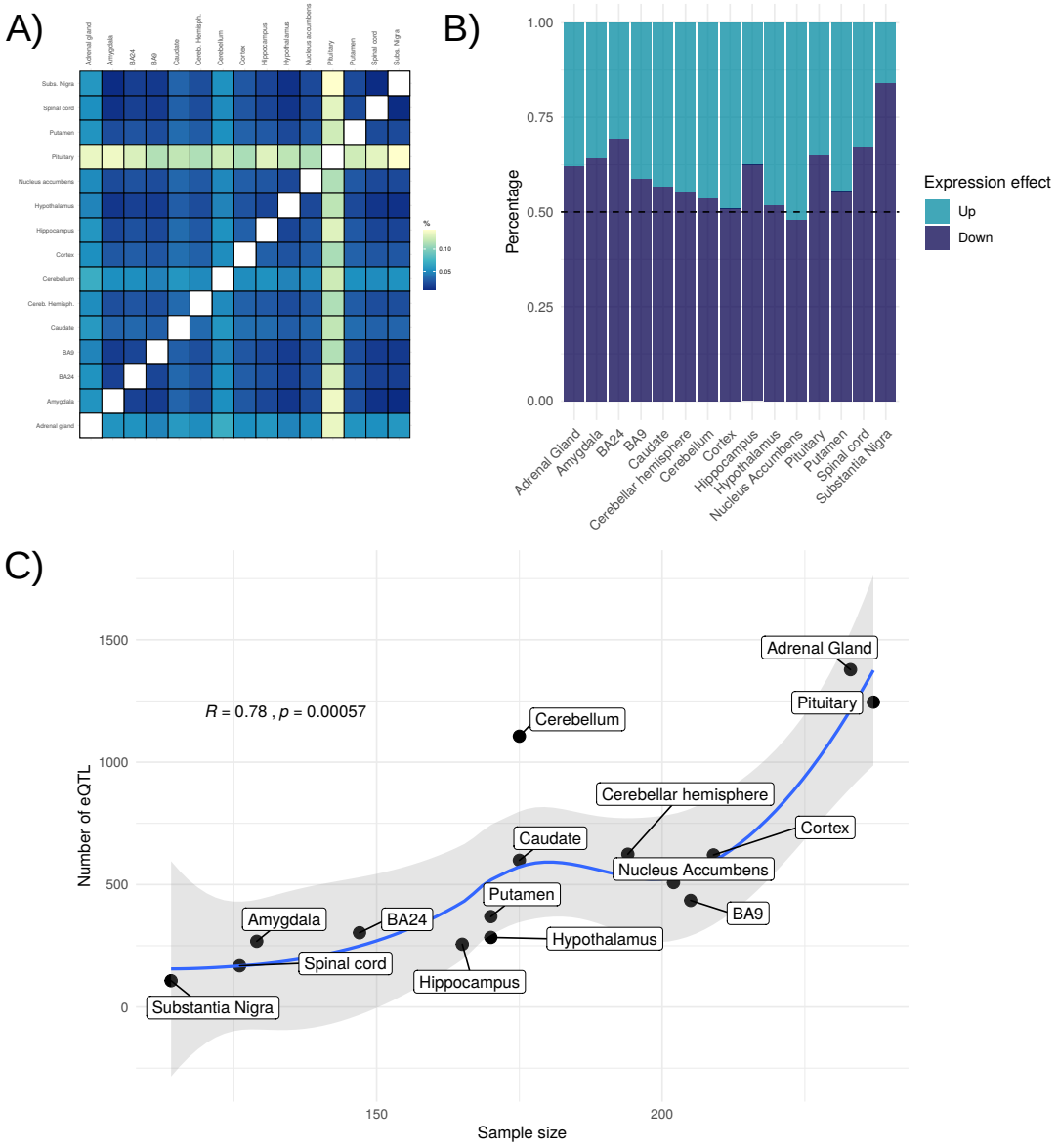

Figure 3: A) Heatmap showing the percentage of eQTL that are unique in each of the tissues B) ratio of normalized effect size in expression in each of the 15 tissues included in the study, and C) distribution of tissues in relation to sample size and unclumped database variants, after filtering for *Homo sapiens* specific frequency, and results (r and p-value) obtained by a Pearson correlation test.